IEEE/CSC & ESAS EUROPEAN SUPERCONDUCTIVITY NEWS FORUM (ESNF), No. 11, January 2010
Published in *Journal of Physics Conf. Series* (*SuST*) **234**, 012017 (2010)

Superconducting nanowire single-photon detectors: Quantum Efficiency vs. thickness of NbN films

M Hofherr[1], D Rall[1], K S Ilin[1], A Semenov[2], N Gippius[3] and H-W Hübers[2] and M Siegel[1]

[1]Institut für Mikro- und Nanoelektronische Systeme, Universität Karlsruhe, Karlsruhe, Germany
[2]DLR Institut für Planetenforschung, Berlin, Germany
[3]LASMEA, CNRS, Universite Blaise Pascal, Aubiere, France

E-mail: m.hofherr@ims.uni-karlsruhe.de

Abstract. The quantum efficiency (QE) of thin NbN superconducting nanowire single-photon detectors (SNSPD) has been systematically studied in a wide spectral range from 400 to 2000 nm radiation wavelength. SNSPDs were made from thin NbN films with thickness between 4 and 12 nm deposited on sapphire substrates. The observed reduction of QE with increasing radiation wavelength is caused by a crossover from the "hot-spot" to the "vortex" mechanism of the nanowire detector response. The crossover wavelength shifts to shorter wavelengths with increasing thickness of NbN films.

1. Introduction

Modern optical applications like correlation spectroscopy and quantum cryptography in telecommunication require fast detectors with ultimate quantum efficiency and spectral resolution in the optical and infrared spectrum range. Superconducting nanowire single-photon detectors (SNSPD) [1] are currently considered as a promising alternative to transition edge sensors [2] and superconducting tunnel-junction detectors [3]. The latter detectors are able to count photons in the near infrared range with resolution of 0.15 eV, but their costs of operation are much higher due to sub-Kelvin temperatures and using of SQUID readout, which additionally limits the count rate of these detectors to hundreds of kilohertz. The SNSPD devices are usually a meander line structure with a width $W < 100$ nm made from a superconducting film with thickness $d < 10$ nm. The detectors made from the most popular NbN films are operated at 4.2 K and biased with current I_{bias} slightly below the critical current value I_C. The SNSPD devices can realize count rates up to 10^8 events per second but the quantum efficiency (QE) of detectors without optical cavity is not more than 10 % [4]. A lot of experimental and theoretical efforts have been applied to understand the particular mechanism of the response of a superconducting nanowire to absorbed photons with different energy [5] - [7]. Nevertheless, some of the theoretical assumptions are not experimentally validated so far and therefore further improvement of the SNSPD performance creates difficulty.

In this paper we report on results of a systematic experimental study of the quantum efficiency of the SNSPD devices made from ultra-thin NbN film. We present and discuss spectra of the detector response measured at different bias conditions and on detectors made from the superconductive NbN films with different thickness. Obtained results allow us to demonstrate a crossover between two

mechanisms of the superconducting nanowire response with increase of the radiation wavelength, i.e. with decrease of the energy of absorbing photons.

2. Thin film fabrication and patterning

The NbN films are fabricated by DC reactive magnetron sputtering from a pure niobium target in an argon/nitrogen atmosphere onto sapphire substrates kept at 750°C during deposition. The thickness of films was varied between 4 and 12 nm. The temperature dependence of resistance $R(T)$ was measured right after deposition and the critical temperature T_C of as deposited films was defined as the zero resistance temperature. We obtained $T_C \approx 16$ K for the thickest film with $d > 10$ nm. A reduction of the thickness below 10 nm results in a gradual decreasing of the critical temperature until about 13 K for the thinnest $d \approx 4$ nm thick NbN film. The observed reduction of T_C with decreasing film thickness is typical for superconducting films with thickness about of the coherence length [8], [9]. The suppression of T_C in such thin films can be described in terms of the proximity effect model [10] – [12] assuming a destruction of superconductivity in the surface and film to substrate interface layers of NbN thin films.

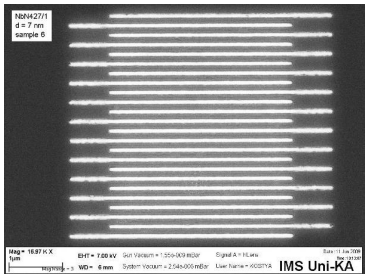

Figure 1. SEM image of a detector area: bright lines are reflections from surface of sapphire substrate and black area is NbN.

The NbN films were patterned into meander line structures with a nominal width $W \approx 90$ nm and a filling factor (ratio of W to the pitch of the meander structure) of about 50 % which covers an area 4 x 3.5 μm^2. The patterning was made by standard electron beam lithography and Ar ion milling technique. The actual dimensions of the detector structure were measured using scanning electron microscopy. A typical SEM image of one of our SNSPD is shown in figure1. Already at this step of device fabrication we made a preliminary selection of detectors that have no visible defects (constrictions, breaks, short circuits, etc.) of meander line. The $R(T)$ dependencies and the current-voltage characteristic at $T = 4.2$ K were measured on all devices after fabrication and the zero critical temperature and the critical current density $j_C(4.2\ \mathrm{K})$ were extracted. We obtained a reduction of $j_C(4.2\ \mathrm{K})$ with thickness of NbN films from about 18 to 5 MA/cm^2 for the thickest (12 nm) and the thinnest (4 nm) film correspondingly. We have to note that the patterning process results in reduction on about 1 K of T_C of our 90 nm wide meander lines with respect to T_C of non-structured films. Nevertheless the lowest T_C of SNSPDs made from the thinnest NbN films was about 11.5 K and the critical current was about 20 μA at 4.2 K resulting in a large signal to noise ration during optical characterization of SNSPD. The meander line is embedded into a coplanar waveguide structure made from the same film to optimize the RF-transmission behavior of the complete readout.

2. Results and discussion.

Experimental set-up

A principle scheme of the experimental set-up is shown in Fig. 2. The measurements were done in an evacuated He^4 bath cryostat at T ≈ 5 K. For calibration purpose, the flux was independently measured at the detector position. A beam generated by a halogen lamp (broad spectrum with 400 nm to 2000 nm wavelength) was passed through a prism monochromator and then directed into the cryostat through a SiO_2 window. The detector was bonded to a microstrip waveguide circuit, which includes a bias-tee to separate DC and AC signals.

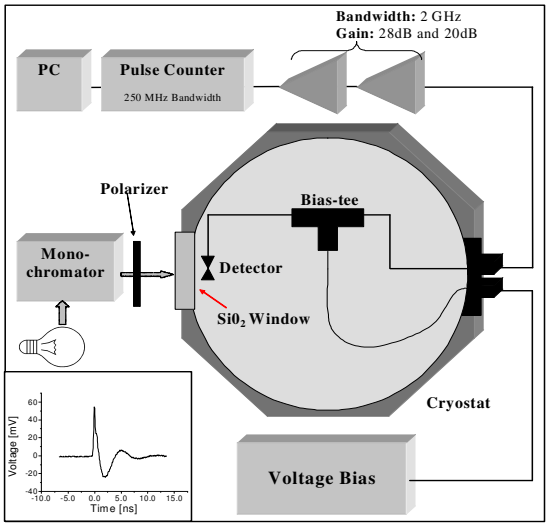

Figure 2. Scheme of experimental set-up. Inset: Example of pulse from SNSPD recorded by 6 GHz - oscilloscope.

The detector was biased with the current to 95 % of its critical current at the operation temperature to get comparable results for all detectors. The bias was provided by a low noise voltage source at the operation temperature to get comparable results for all detectors. The output signal was guided out of the cryostat by a coaxial cable and amplified by two rf-amplifiers in series (total gain is 50 dB, bandwidth is 2 GHz). The pulse rate was measured with a PC controlled SR400 pulse counter with 5 ns time resolution.

Quantum Efficiency: Dependence on bias current

Figure 3 shows spectra of the quantum efficiency of a 5.7 nm thick film measured at different bias conditions between 0.7 and 0.95 of the critical current value. For bias currents close to I_C the quantum efficiency is independent of photon energy over a wide wavelength range. Starting from about 700 nm (the roll-off wavelength indicated by the arrow in figure 3), the quantum efficiency decreases monotonically with increasing wavelength.

For lower bias currents the roll-off wavelength shifts to shorter wavelengths and for $I_{bias} = 0.7\ I_C$ the plateau in the QE dependence on wavelength disappears almost completely. The spectrum obtained at the lowest bias current $0.7\ I_C$ shows a second plateau in the infrared range caused by the limit of sensitivity of our measurement setup.

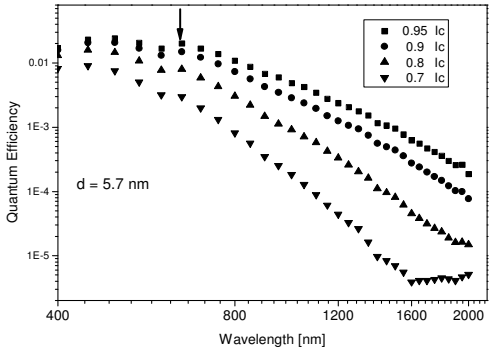

Figure 3. Dependence of the quantum efficiency on radiation wavelength measured at different bias current values indicated in the graph. The arrow marks the roll-off wavelength for $I_{bias} = 0.95\ I_c$.

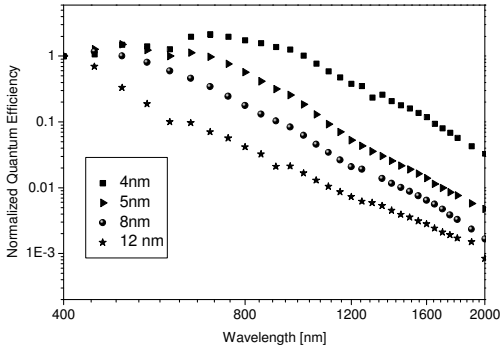

Figure 4. Spectra dependence of the normalized quantum efficiency of SNSPDs made from NbN films with different thicknesses indicated in the graph.

It is known [13] that at biasing conditions very close to I_C the contribution to QE from dark counts becomes more and more significant. Therefore the dependence of the dark count rate on bias current was independently measured for each sample in the same experimental setup. The dark count rate was than subtracted from the measured count rate.

Quantum Efficiency: Dependence on thickness

Figure 4 shows the normalized QE of SNSPDs with different thickness of NbN films indicated in the graph. All SNSPDs were measured at $I_{bias} = 0.95\, I_C$. The device made from 4 nm thick NbN film shows a plateau in its spectrum up to about $\lambda \approx 900$ nm. For longer wavelengths the value of quantum efficiency decreases gradually. It is seen in Fig. 4 that the roll-off wavelength shifts to shorter λ values with increase of the NbN film thickness. For SNSPDs made from 12 nm thick NbN film the QE spectrum does not reveal any plateau and its value reduces monotonically starting from the shortest wavelength of our measurements.

The slight increase of the QE of the 4 nm thick SNSPD which can be seen right before roll-off is due to the non-monotonic spectra dependence of absorbance of the meander line [14]. The absorbance is found to be one of the main limiting factors of the SNSPD quantum efficiency. It depends on the thickness of superconducting NbN film and on the energy of absorbed photons. The spectral dependence of the quantum efficiency of SNSPD on bias current and on thickness of NbN film indicates that there are two different detection mechanisms realized in superconductive nanowires. At optical and near UV wavelengths (plateau regions in Fig. 3 and 4), the response of the detectors can be described as follows: a photon absorbed somewhere in the nanowire produces a non-equilibrium hot-spot with reduced concentration of Cooper pairs. The detector is current-biased by the current I_{bias} close to but less than the critical current I_C. The remaining Cooper pairs in the hot-spot have to accelerate in order to carry the applied bias current. Once the velocity of Cooper pairs reaches the critical value, the superconductivity over the entire cross-section of the wire breaks down and a normal-conducting domain is formed giving rise to a voltage transient between the wire ends. The dynamic behavior of this normal domain is mainly influenced by the current as it has been shown in [15].

The normal domain formation should be limited to large photon energies where the exact boundary obviously depends on the cross-section of the wire $W*d$ [16]. The microscopic analysis gives the following criterion for the minimum photon energy required for the formation of the normal domain:

$$h\nu = \frac{N_0 \Delta^2 W d\, \xi}{2}\left(1 - \frac{I_{bias}}{I_C}\right), \qquad (1)$$

where N_0 is the electron density of states at the Fermi level, Δ is the superconducting energy gap, ξ is the coherence length and I_C is the critical current. At wavelengths, larger than λ, corresponding to this photon energy, an abrupt drop of the detection efficiency is expected [17] if only the "hot-spot" detection mechanism determines the response of the superconducting nanowire. Photons with energies, equal or higher than the energy defined by (1) cause a maximum count rate independent of the photon energy thus resulting in plateau in spectra shown in Fig. 3 and 4.

The mechanism responsible for detection photons with energies lower than (1), is still under investigation. It is obvious that due to limitation (1) the photon energy is not enough to cause a formation of the normal domain and therefore a voltage pulse across the nanowire. The "vortex" assistant model is currently considered to be one of possible mechanism describing the response of SNSPD in the forbidden part of spectra. In spite of the very small width of superconducting strips used for SNSPD development, they are still wider than Likharev's limit [18]. Thus there is a non-zero probability for penetration of magnetic vortices into the strip. This probability can be enhanced by the absorbed photon which effectively suppresses a potential barrier for vortex penetration. The detector is biased with current thus the Lorentz force will act immediately on the penetrated vortex. Since I_{bias} of

SNSPD is about the critical current value the vortices can be de-pinned and starts to cross the strip thus producing the voltage pulse.

3. Conclusion

The quantum efficiency of superconducting nanowire single photon detectors made from NbN films width thickness between 4 and 12 nm has been measured in a wide spectral range from 400 to 2000 nm wavelength. Two parts in the QE spectra can be distinguished: A plateau at short wavelengths and gradual reduction of QE for the wavelengths longer than the roll-off wavelength. The value of this roll-off wavelength shifts to the UV part of spectra with decrease of the bias current and increase of thickness of NbN films according to theoretical predictions (1). The response of SNSPD at photon energies larger than (1) is well described by the "hot-spot" model. The mechanism responsible for the gradual reduction of the QE values with increase of radiation wavelength is probably caused by the photon assistant penetration of magnetic vortices into superconducting nanowire and their dynamics under influence of the Lorentz force.

References

[1] Semenov A D, Gol'tsman G N, Korneev A A, 2001, *Physica C*, **351**, pp. 349-356.

[2] Cabrera B, Martinis J M, Miller A J, Nam S W, Romani R, *AIP Conference Proceedings*, 2002, **605**, pp. 565-570

[3] Fraser G W, Heslop-Harrison J S, Schwarzacher T, Holland A D, Verhoeve P, Peacock A, 2003, *Review of Scientific Instruments*, **74**, pp. 4140-4144, 2003

[4] Semenov A D, Haas P, Günther B, Hübers H-W, Il'in K and Siegel M 2007, Supercond. Sci.Technol. **20**, 919-924

[5] Semenov A D, Nebosis R S, Gousev Yu P, Heusinger M A and Renk K F 1995**,** *Physical Review B (Condensed Matter)*, **52**, Issue 1, pp.581-590

[6] Engel A, Semenov A, Hübers H-W, Il'in K and Siegel M 2004, *Journal of Modern Optics*, **51**, 9,1459 - 1466

[7] Gol'tsman G N, Okunev O, Chulkova G, Lipatov A, Semenov A, Smirnov K, Voronov B and Dzardanov A 2001, *Appl. Phys. Lett.* **79**, No. 6

[8] Wolf S A, Rachford F J and Nisenoff M 1978, *J. Vac. Sci. Technol.* **15**(2), pp. 386-388

[9] Park S I and Geballe T H 1985*, Physica,* **135B**, pp. 108-112,

[10] Cooper L N 1961, *Phys. Rev. Lett*., **6**, pp. 689-690

[11] Fominov Ya V and Feigel'man M V 2001, *Phys. Rev. B*, **63**, 094518

[12] Il'in K, Schneider R, Gerthsen D, Engel A, Bartolf H, Schilling A, Semenov A, Hübers H-W, Freitag B, and Siegel M 2008, *Journal of Physics*: Conference Series **97**, 012045, 2008. DOI: 10.1088/1742-6596/97/1/012045

[13] Semenov A, Engel A, Il'in K, Siegel M, and Hübers H-W, IEEE Transaction on Applied Superconductivity, **15**, 2, 518- 521, 2005.

[14] Semenov A, Günther B, Böttger U, Hübers H-W, Bartolf H, Engel A, Schilling A, Il'in K, Siegel M, Schneider R, Gerthsen D, and Gippius N A 2009, Phys. Rev. B **80**, 054510.

[15] Semenov A D, Haas P, Hübers H-W, Il'in K, Siegel M, Kirste A, Drung D, Schurig T and Engel A 2009, *Journal of Modern Optics*, **56**, Issue 2 & 3, pages 345 - 351

[16] Semenov A, Engel A, Hübers H-W, Il'in K and Siegel M 2005, *The European Phys. Journal B*, **47**, pp. 495-501

[17] Semenov, A, Engel A, Il'in K, Gol'tsman G, Siegel M and Hübers H-W 2003, *Eur. Phys. J.* AP **21**, 171-178

[18] Likharev K K, 1997, *Rev. Mod. Phys.* **51**, 1, 101-159